JACS
JOURNAL OF THE AMERICAN CHEMICAL SOCIETY
pubs.acs.org/JACS
Article

# Alternating Isotactic Polyhydroxyalkanoates via Site- and Stereoselective Polymerization of Unsymmetrical Diolides

Zhen Zhang, Changxia Shi, Miriam Scoti, Xiaoyan Tang, and Eugene Y.-X. Chen*

Cite This: J. Am. Chem. Soc. 2022, 144, 20016−20024
Read Online



**ABSTRACT:** Naturally produced, biodegradable polyhydroxyalkanoates (PHAs) promise more sustainable alternatives to nonrenewable/degradable plastics, but biological PHA's stereomicrostructures are strictly confined to isotactic (*R*)-polymers or copolymers of random sequences. Chemical synthesis via catalyzed ring-opening polymerization (ROP) of cyclic (di)esters offers expedient access to diverse PHA microstructures, including those with defined comonomer sequences and tacticities. However, the synthesis of alternating isotactic PHAs has not been achieved by the existing methodologies. Here, we report the design of unsymmetrically disubstituted eight-membered diolides (*rac*-8DL$^{R1\text{-}R2}$) and their site- and stereoselective ROP with discrete chiral catalysts, enabling the synthesis of alternating isotactic PHAs, poly(3-hydroxybutyrate-*alt*-3-hydroxyvalerate) (*alt*-P3HBV) and poly(3-hydroxybutyrate-*alt*-3-hydroxyheptanoate) (*alt*-P3HBHp), with high to quantitative (>99%) alternation and isotacticity and $M_n$ up to 113 kDa and $Đ$ = 1.01. Physical properties of such PHAs are substantially determined by the degree of backbone sequence alternation and tacticity, ranging from amorphous to semi-crystalline materials. The *alt*-P3HBV shows significantly improved mechanical performance relative to the constituent homopolymers. Intriguingly, enantiomeric (*R*)-*alt*-P3HBV and (*S*)-*alt*-P3HBV, synthesized by kinetically resolved ROP of *rac*-8DL$^{Me\text{-}Et}$, form a stereocomplex with a significantly enhanced $T_m$ (by 53 °C), while the enantiomeric homopolymers do not form a stereocomplex.

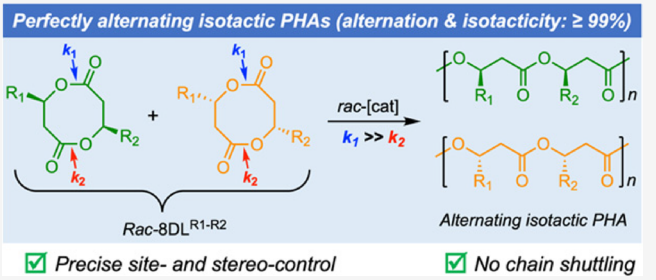


## INTRODUCTION

Polyhydroxyalkanoates (PHAs) belong to a large family of biodegradable and biocompatible aliphatic polyesters that possess diverse properties and thus applications in biomedical, pharmaceutical, and packaging areas, the last of which holds great potential to partially substitute conventional non-degradable plastics.[1−11] To tune the properties, PHAs built from various (co)monomers polymerized by diverse catalysts have been prepared.[12−20] A different approach to modulate the properties of PHAs, and thus broaden the potential applications, is through manipulating the sequence of the repeating units along the polymer backbone or controlling the tacticity of polymer chains,[21−26] which can be achieved through catalyzed ring-opening polymerization (ROP) by catalyst-site−controlled coordination polymerization.[27−32] For example, 60+ years of research in pursuing chemical synthesis of microbial poly(3-hydroxybutyrate) (P3HB), which is a purely isotactic polymer, has recently culminated in a metal-catalyzed ROP of eight-membered racemic dimethyl diolide (*rac*-8DL$^{Me}$) to perfectly isotactic P3HB with *meso* triad [*mm*] > 99%, number-average molecular weight ($M_n$) = 154 kDa, dispersity ($Đ$) = 1.01, and melting-transition temperature ($T_m$) = 171 °C.[33] Catalyzed chemical synthesis of enantiomeric (*R*)-P3HB and (*S*)-P3HB with $T_m$ = 175 °C has also been realized via enantioselective polymerization of *rac*-8DL$^{Me}$.[33] Syndiotactic P3HB with $P_r$ (probability of racemic linkages between monomer units) up to 94% was also synthesized by Carpentier et al. through ROP of *rac*-*β*-butyrolactone (*rac*-*β*-BL) using yttrium complexes supported by dianionic aminoalkoxybis(phenolate) ligands.[34,35] Through the ROP of 8DL$^{Me}$ diastereomeric mixtures, isotactic-*b*-syndiotactic sequenced P3HB has also been created.[36] Taking advantage of chain-end control, in which the stereogenic center of (essentially) the last inserted monomer biases the catalyst to selectively incorporate the next monomer with the opposite stereoconfiguration, Coates et al. employed two sets of enantiomeric *β*-lactones with opposite absolute stereoconfigurations using syndiospecific bimetallic yttrium complexes supported by tetradentate phenoxyamine ligands, affording alternating syndiotactic PHA copolymers (alternation up to 94%) with interesting physical properties distinct from individual homopolymers or random copolymers (Scheme 1).[13] Follow-

Received: August 18, 2022
Published: October 18, 2022

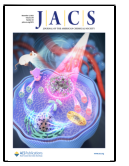

**Scheme 1. Synthesis of Alternating Stereoregular PHAs**[a]

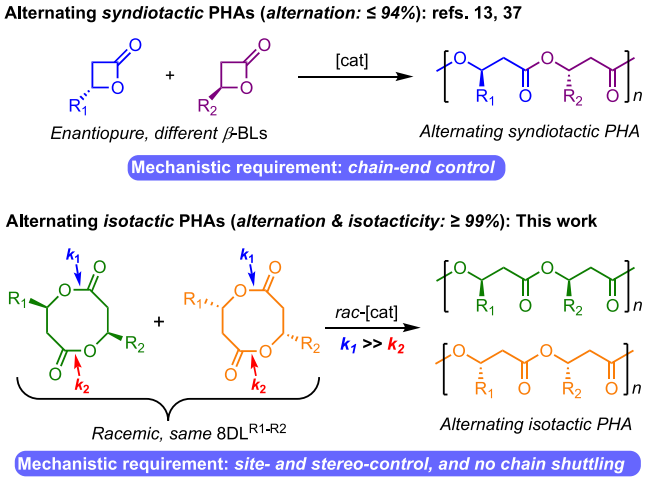


[a]Comparison between alternating syndiotactic PHAs using two enantiopure, different β-BLs and alternating isotactic PHAs using the same diolide, *rac*-8DL$^{R1-R2}$.

ing this chain-end-control methodology, alternating syndiotactic copolymerization of allyl and benzyl β-malolactonates was realized using an yttrium complex supported by a tetradentate dichloro-substituted bis(phenolate) ligand, and the resulting copolymers are readily post-functionalizable through hydrogenolysis of the benzyloxycarbonyl or functionalization of the allyl pendant groups, offering a new class of alternating syndiotactic copolymers with designed functional groups.[37] However, when such a mixture of (*R*) and (*S*)-lactones was subjected to copolymerization by isoselective catalysts, a mixture of isotactic homopolymers, rather than envisioned alternating isotactic copolymers, was produced.[14]

Naturally, a fundamental question is how to create alternating isotactic PHA copolymers, where the backbone carbon atoms have the same absolute configuration but with alternating substituent groups. Here, the chain-end-control method, which alternatively enchains monomers with opposite stereogenic centers, apparently did not work.[14] Another approach to prepare alternating copolyesters is to utilize unsymmetric cyclic diesters. For example, alternating poly(lactic-*co*-glycolic acid) was synthesized via a regioselective ROP of (*S*)-methyl glycolide catalyzed by an enantiomeric aluminum salen catalyst with the binaphthyl backbone.[38] Similarly, an alternating isotactic copolymer of lactic acid and mandelic acid was successfully synthesized by polymerizing enantiomerically pure methyl-6-phenyl-1,4-dioxane-2,5-dione (MPDD) with a *rac*-methyl lactate TMP−Zn complex (TMP = 1,5,9-trimesityldipyrromethene);[39] an alternating heterotactic copolymer was also synthesized by regio- and stereoselective polymerization of *rac*-MPDD. Inspired by these results, we hypothesized that alternating isotactic PHAs could be generated from unsymmetrically disubstituted *rac*-8DLs that possess two stereogenic centers with the same stereoconfiguration yet different alkyl groups ($R_1$-$R_2$, Scheme 1). Differing from the prior work where only one of the two sequence-control factors, that is, stereoselectivity (for the chain-end-control method) and regioselectivity (for the ROP of enantiopure diesters), needs to be addressed during the polymerization, creation of novel alternating isotactic PHAs from the unsymmetric *rac*-8DLs strictly requires *simultaneous control of both stereoselectivity and site selectivity* during the ring-opening processes; otherwise, both stereo- and regio-sequence errors could take place individually or concurrently. Excitingly, by judiciously choosing the catalyst and reaction conditions, perfectly alternating isotactic PHA copolymers, poly(3-hydroxybutyrate-*alt*-3-hydroxyvalerate) (*alt*-P3HBV) and poly(3-hydroxybutyrate-*alt*-3-hydroxyheptanoate) (*alt*-P3HBHp), were obtained through kinetically resolved, stereoselective ROP of unsymmetric *rac*-8DLs (Scheme 1). The alternating isotactic PHAs displayed significantly different thermal properties (crystallization processes, thermal transitions, and physical states) relative to their homopolymers, which are closely related to the percentage of backbone alternation and stereoregularity. In sharp contrast to the individual isotactic homopolymers, which are brittle with an ultimate tensile strain less than 10%, *alt*-P3HBV exhibits much improved mechanical properties with an elongation at break reaching 220%. By using enantiopure catalysts, enantiomeric PHAs, (*R*)-*alt*-P3HBV and (*S*)-*alt*-P3HBV, were also synthesized through site- and enantioselective ROP, and surprisingly, they were able to form a stereocomplex showing a significantly enhanced $T_m$. In contrast, this stereocomplexation behavior is absent in their isotactic homopolymers.

## RESULTS AND DISCUSSION

**Site- and Stereoselective ROP of *RR/SS*-8DL$^{Me-Et/Bu}$.** The diolide monomer unsymmetrically disubstituted with methyl and ethyl groups in its racemic form, *RR/SS*-8DL$^{Me-Et}$, was synthesized from bio-sourced dimethyl succinate, as outlined in Scheme S1. Although the overall synthetic scheme follows that of the general synthetic protocol for the symmetrically disubstituted diolides,[33,36] step-wise installation of the Me and Et groups via alkylation by MeI (first) and EtI (second) was required for the synthesis of *RR/SS*-8DL$^{Me-Et}$. Spectroscopic analysis and single-crystal X-ray diffraction (SC-XRD) study confirmed its formation, purity, and absolute configuration (Figures 1A and S1−S12). The methyl- and *n*-butyl-substituted diolide derivative, *RR/SS*-8DL$^{Me-Bu}$, was synthesized in the same fashion (Scheme S1).

Given that undesired inter-/intrachain transesterification commonly takes place in the ROP of cyclic esters catalyzed by either organic bases or metal-based complexes,[40−42] which would scramble polymer backbones and lead to sequence errors, we first employed matrix-assisted laser desorption/

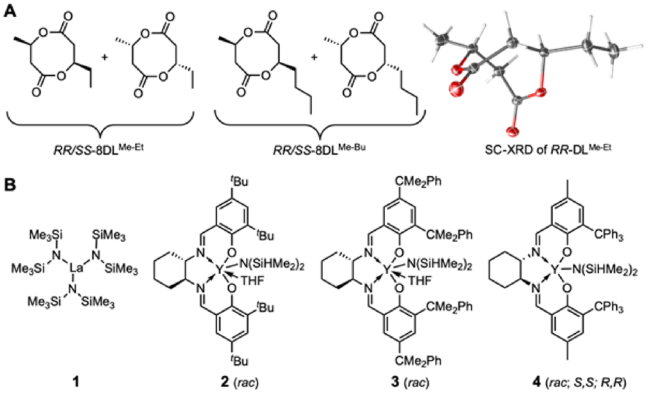


**Figure 1.** (A) Chemical structures of the unsymmetric *rac*-8DLs synthesized in this work and crystal structure of *RR*-8DL$^{Me-Et}$ obtained via SC-XRD. (B) Metal-based achiral (**1**), $C_2$-chiral racemic (**2**−**4**), and enantiomeric (*R*,*R*- and *S*,*S*-**4**) catalysts employed in this study.


https://doi.org/10.1021/jacs.2c08791
J. Am. Chem. Soc. 2022, 144, 20016−20024

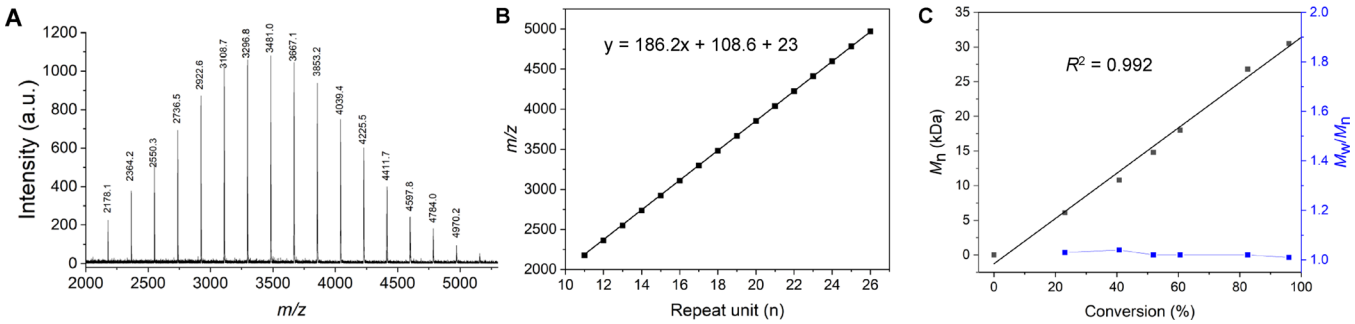


**Figure 2.** (A) MALDI-TOF MS spectrum of isotactic *alt*-P3HBV prepared with [*RR*/*SS*-8DL$^{Me\text{-}Et}$]/[**4**]/[BnOH] = 20/1/1. (**B**) Plot of $m/z$ values ($y$) versus the theoretical number of the *RR*/*SS*-8DL$^{Me\text{-}Et}$ repeating unit ($x$). (C) $M_n$ and $Đ$ values (measured by GPC in THF) as a function of monomer conversion for the polymerization with [*RR*/*SS*-8DL$^{Me\text{-}Et}$]/[**4**]/[BnOH] = 100/1/1.

**Table 1. Selected Results of Polymerization of *RR*/*SS*-8DL$^{Me\text{-}Et/Bu}$ under Various Reaction Conditions[a]**

| run | monomer | catalyst | [M]/[cat] | temp. (°C) | time (min) | conv.[b] (%) | $M_n$[c] (kDa) | $M_{n\ calcd}$ (kDa) | $Đ$[c] ($M_w/M_n$) | % of[d] alternation |
|---|---|---|---|---|---|---|---|---|---|---|
| 1 | (±)-DL$^{Me\text{-}Et}$ | **1** | 20/0.33 | 25 | 30 | 56.5 | 5.60 | 2.21 | 1.82 | 70.3 |
| 2 | (±)-DL$^{Me\text{-}Et}$ | **2** | 20/1 | 25 | 30 | 100 | 15.6 | 3.83 | 1.03 | |
| 3 | (±)-DL$^{Me\text{-}Et}$ | **2** | 200/1 | 25 | 30 | 100 | 61.0 | 37.4 | 1.02 | 78.2 |
| 4 | (±)-DL$^{Me\text{-}Et}$ | **3** | 100/1 | 25 | 30 | 100 | 29.6 | 18.7 | 1.04 | |
| 5 | (±)-DL$^{Me\text{-}Et}$ | **3** | 200/1 | 25 | 30 | 100 | 49.6 | 37.4 | 1.09 | 79.6 |
| 6 | (±)-DL$^{Me\text{-}Et}$ | **3** | 400/1 | 25 | 30 | 100 | 119 | 74.6 | 1.30 | |
| 7 | (±)-DL$^{Me\text{-}Et}$ | **4** | 20/1 | 25 | 1 | 100 | 6.50 | 3.83 | 1.19 | |
| 8 | (±)-DL$^{Me\text{-}Et}$ | **4** | 100/1 | 25 | 15 | 100 | 19.2 | 18.7 | 1.01 | |
| 9 | (±)-DL$^{Me\text{-}Et}$ | **4** | 200/1 | 25 | 30/600 | 66/73 | 30.7 | 27.3 | 1.01 | >99 |
| 10 | (±)-DL$^{Me\text{-}Et}$ | **4** | 200/1 | 55 | 600 | 66 | 24.6 | 24.7 | 1.01 | |
| 11 | (±)-DL$^{Me\text{-}Et}$ | **4** | 200/1 | 0 | 600 | 86 | 31.7 | 32.1 | 1.01 | |
| 12 | (±)-DL$^{Me\text{-}Et}$ | **4** | 200/1 | −30 | 30 | 100 | 40.6 | 37.4 | 1.01 | >99 |
| 13 | (±)-DL$^{Me\text{-}Et}$ | **4** | 400/1 | −30 | 600 | 65 | 33.0 | 48.5 | 1.01 | |
| 14[e] | (±)-DL$^{Me\text{-}Et}$ | **4** | 200/1 | −30 | 720 | 100 | 113 | 149 | 1.01 | |
| 15 | (±)-DL$^{Me\text{-}Et}$ | (*R*,*R*)-**4** | 200/1 | −30 | 30 | 50 | 32.4 | 18.7 | 1.02 | |
| 16 | (±)-DL$^{Me\text{-}Et}$ | (*S*,*S*)-**4** | 200/1 | −30 | 30 | 50 | 30.9 | 18.7 | 1.01 | |
| 17 | (±)-DL$^{Me\text{-}Bu}$ | **2** | 100/1 | 25 | 30 | 100 | 50.5 | 21.5 | 1.06 | 74.2 |
| 18 | (±)-DL$^{Me\text{-}Bu}$ | **2** | 200/1 | 25 | 30 | 64.6 | 24.1 | 27.8 | 1.12 | |
| 19 | (±)-DL$^{Me\text{-}Bu}$ | **3** | 100/1 | 25 | 30 | 100 | 31.4 | 21.5 | 1.06 | 75.2 |
| 20 | (±)-DL$^{Me\text{-}Bu}$ | **3** | 200/1 | 25 | 30 | 45.6 | 22.0 | 19.6 | 1.03 | |
| 21 | (±)-DL$^{Me\text{-}Bu}$ | **4** | 100/1 | 25 | 30 | 70.7 | 18.5 | 15.3 | 1.04 | >99 |

[a]Reaction condition: [M] = 1.0 M, toluene as the solvent, benzyl alcohol (BnOH) as the initiator, [catalyst]/[BnOH] = 1:3 for **1** and 1:1 for **2**, **3**, and **4**, catalyst and BnOH premixed in toluene at room temperature (~25 °C) before adding into the monomer solution. The racemic monomers, *RR*/*SS*-8DL$^{Me\text{-}Et/Bu}$, were abbreviated as (±)-DL$^{Me\text{-}Et/Bu}$ for clarity. Note: the polymerization in dichloromethane behaved similarly. [b]Conversions of monomers measured by $^1$H NMR spectra of the quenched solution in benzoic acid/chloroform. [c]Weight-average molecular weight ($M_w$), number-average molecular weight ($M_n$), and dispersity ($Đ = M_w/M_n$) determined by GPC coupled with an 18-angle light scattering detector at 40 °C in chloroform. [d]The percentage of alternation was determined from integration at the carbonyl region of the semi-quantitative $^{13}$C NMR spectrum. [e][catalyst]/[BnOH] = 1:0.25. Note: the initiation efficiency = $M_n$(calcd)/$M_n$(exptl), where $M_n$(calcd) = MW((±)-DL$^{Me\text{-}Et/Bu}$) × [(±)-DL$^{Me\text{-}Et/Bu}$]/[BnOH] × conv (%) + MW of chain-end groups (BnOH) = 186.21 (214.26) × [(±)-DL$^{Me\text{-}Et/Bu}$]/[BnOH] × conv (%) + 108.14.

ionization time-of-flight mass spectroscopy (MALDI-TOF MS) to gain an insight into the microstructure of the PHAs produced by the employed catalysts (Figure 1B) in a ratio of [monomer]/[catalyst]/[BnOH] = 20:1:1. It was found that if the polymerization was quenched at or before full monomer conversion, no transesterification was observed (Figures 2A, S13, and S14), as indicated by the mass spectrum showing exclusive molecular ion peaks with a spacing of 186.2 corresponding to the whole ring-opened *RR*/*SS*-8DL$^{Me\text{-}Et}$ repeating unit (Figure 2B). This well-behaved ROP feature is the same as that observed for the ROP of symmetrically disubstituted diolides.[33,36]

The scaled-up ROP of *RR*/*SS*-8DL$^{Me\text{-}Et}$ was initially screened with La[N(SiMe$_3$)$_2$]$_3$ (**1**), which was previously demonstrated to be an effective catalyst to polymerize lactones.[43−45] With the BnOH initiator and [monomer]/[**1**]/[BnOH] = 20:0.33:1 (Table 1, run 1), the polymerization in toluene at room temperature (~25 °C) led to a conversion of 56.5% in 30 min. Extending the reaction to 120 min only slightly improved the conversion to 60.2%, yielding a polymer with a low $M_n$ of 5.6 kDa and a high dispersity of $Đ$ = 1.82. Furthermore, $^{13}$C NMR spectra (Figure 3A-a) indicate poor site- and stereo-controls as multiple peaks were observed in the carbonyl region from 169.1 to 169.7 ppm. It is worth noting that a detailed assignment of the individual carbonyl peaks for the polymer produced by **1** is infeasible because **1** exhibits poor stereoselectivity for the ROP of *rac*-8DLs[33] and likely


https://doi.org/10.1021/jacs.2c08791
J. Am. Chem. Soc. 2022, 144, 20016−20024

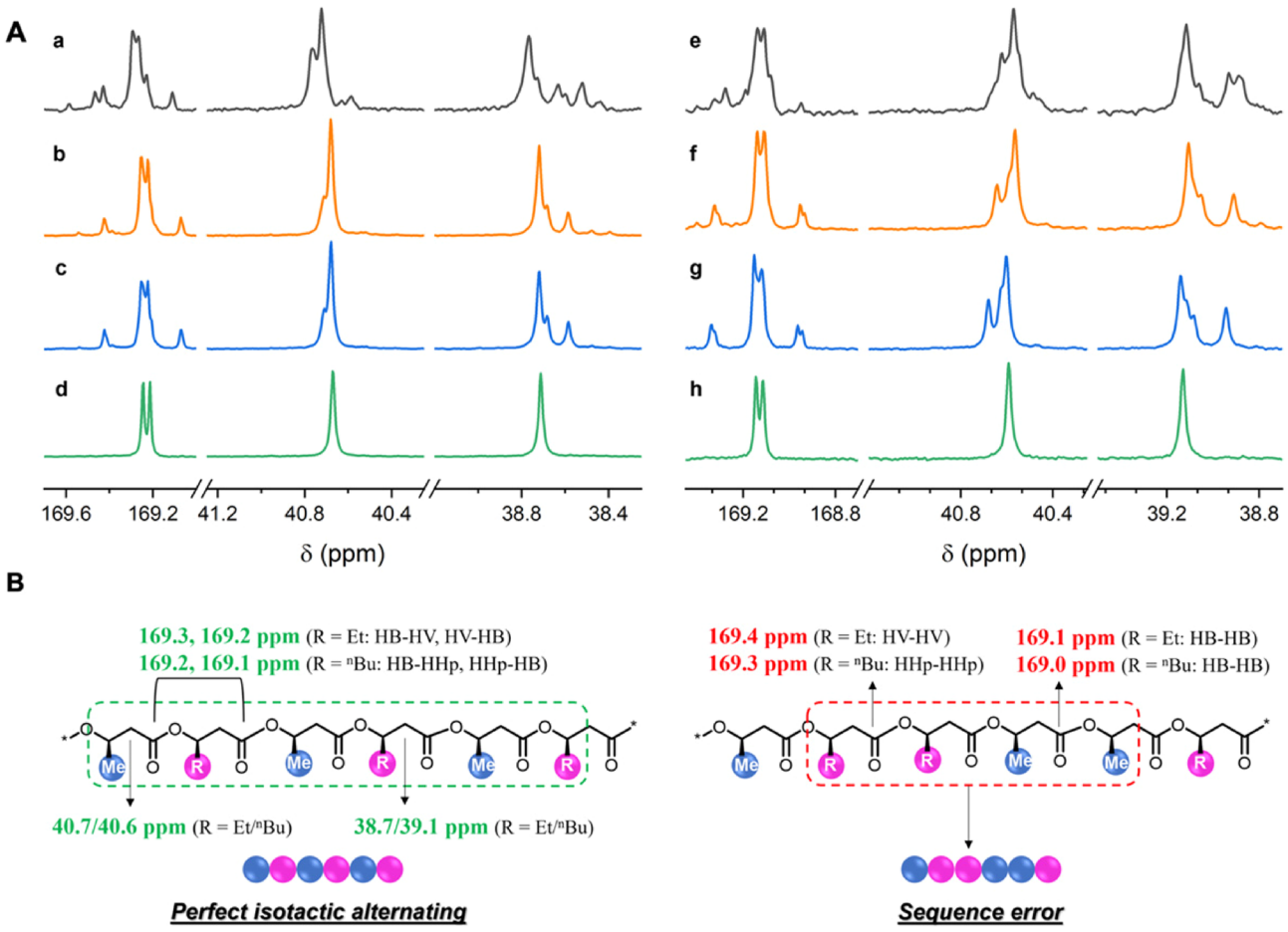


**Figure 3.** (A) $^{13}C$ NMR spectra ($CDCl_3$) of *alt*-P3HBV (a–d) and *alt*-P3HBHp (e–h) prepared with catalysts **1**–**4**, respectively, in the carbonyl and methylene regions. (B) Illustration of perfect isotactic and sequence error-containing *alt*-P3HBV(Hp) backbones with assigned $^{13}C$ NMR chemical shifts. Given the complexity of stereo-mixed sequence errors and the fact that catalysts **2** and **3** mainly caused site-selective errors, stereoselective errors are not shown here.

poor site selectivity as well, which significantly complicated assignments of the carbonyl resonances.

On the basis of our prior work on the ROP of *rac*-8DL$^{Me}$,[33,36] discrete yttrium silylamido complexes supported by *N*,*N*′-bis(salicylidene)cyclohexanediimine (salcy) ligands[33,46,47] exhibit high polymerization activity and efficiency toward 8DLs. Complex **2** with the classic salen ligand bearing the 3,5-di-*tert*-butyl substituents was examined first for its reactivity and regio-/stereoselectivity toward the ROP of *RR*/*SS*-8DL$^{Me-Et}$. Complete polymerization was achieved in 30 min under identical conditions to those employing catalyst **1** (Table 1, run 2). Increasing the monomer loading to 200 equiv still achieved a full monomer conversion in 30 min, leading to an increased $M_n$ to 61.0 kDa with a narrow dispersity $Đ$ = 1.02 (Table 1, run 3). $^{13}C$ NMR spectra (Figure 3A-b) of the resulting polymer displayed a much cleaner carbonyl region showing two main peaks centered at 169.2 ppm from the carbonyls of the isotactic alternating [HB–HV and HV–HB] sequences and two minor peaks at 169.1 and 169.4 ppm, caused by site-selective error during the ROP process that leads to the formation of HB–HB and HV–HV linkages as homopolymer sequence errors (Figure 3B), which is consistent with the carbonyl chemical shifts of the isotactic P3HB and P3HV homopolymers.[33,36] To further enhance the site selectivity regulated by the steric interplay and matching between *RR*/*SS*-8DL$^{Me-Et}$ monomer and catalysts, complex **3** supported by the bulkier cumyl-substituted ligand was employed, but the ROP (Table 1, runs 4–6) did not enhance the degree of isotactic alternation, as compared to complex **2** (Figure 3A-c). It is worth noting that catalyst **3** exhibits excellent activity in the ROP of *RR*/*SS*-8DL$^{Me-Et}$; with a 0.25 mol % catalyst loading, the ROP achieved 100% monomer conversion in 30 min, yielding a high molecular weight *alt*-P3HBV with $M_n$ = 119 kDa (Table 1, run 6). Finally, we arrived at the even bulkier trityl ($Ph_3C$) substituted complex **4** that was previously shown to produce perfect isotactic P3HB.[33] When combining with 1 equiv of BnOH initiator, complex **4** effectively polymerized 20 to 100 equiv of *RR*/*SS*-8DL$^{Me-Et}$ to completion within 15 min at 25 °C (Table 1, runs 7 and 8). The control of the polymerization was demonstrated by monitoring the $M_n$ value as a function of monomer conversion for the polymerization by **4**. As shown in Figure 2C, the molecular weight of the resulting *alt*-P3HBV increased linearly ($R^2$ = 0.992), while all the $Đ$ values from low to high conversions remained low in a narrow range from 1.01 to 1.04. Remarkably, the obtained polymer now displayed *perfect isotactic alternation* as reflected by its $^{13}C$ NMR spectrum that shows only two carbonyl peaks centered at 169.3 ppm and two single methylene carbon peaks at 40.7 and 38.7 ppm that are from the methylene carbons adjacent to methyl/carbonyl and ethyl/carbonyl, respectively (Figure 3A-d,B). These assignments are again consistent with the chemical shifts of


https://doi.org/10.1021/jacs.2c08791
J. Am. Chem. Soc. 2022, 144, 20016–20024

the previous reported homopolymers[1,33,36] and alternating syndiotactic polymers.[13] Higher molecular weight *alt*-P3HBV can be produced with increasing the monomer loading to 200 equiv ($M_n$ = 30.7 kDa, $Đ$ = 1.01, Table 1, run 9), but the reaction did not go to completion at 25 °C. Compared to our previous studies,[33,36] the unsymmetrical *RR*/*SS*-8DL$^{Me-Et}$ polymerized faster than symmetrical *rac*-8DL$^{Et}$ but slower than *rac*-8DL$^{Me}$, indicating that the monomer reactivity is largely affected by the steric hindrance. Catalyst-site-controlled coordination ROP has often shown temperature-dependent reaction extents and rates related to the polymerizability of the monomers and/or the catalyst reactivity under different temperatures.[43,48,49] Performing the ROP of *RR*/*SS*-8DL$^{Me-Et}$ by **4** at 55 °C did not improve the monomer conversion, but the ROP at 0 °C enhanced conversion to 86% (runs 10 and 11). Further decreasing the temperature to −30 °C achieved 100% conversion in 30 min, producing *alt*-P3HBV with $M_n$ = 40.6 kDa, $Đ$ = 1.01 (Table 1, run 12). Moreover, the molecular weight can be further improved to 113 kDa by changing the [catalyst]/[BnOH] ratio to 1:0.25 (Table 1, run 14). Although variable conversions were achieved at different temperatures, the resulting polymers all displayed a narrow dispersity of 1.01 (Table 1, runs 9−12) and the measured $M_n$ values were close to the theoretical ones (the calculated initiation efficiencies ranging from 89 to 101%), indicating a controlled polymerization. The observation of higher monomer conversion at lower temperature is possibly caused by the active species instability at elevated temperature and/or minute residual impurities in the monomers which may have an alleviated impact on the polymerization at lower temperature.

The methodology for the successful synthesis of *alt*-P3HBV can be readily extended to the synthesis of perfectly alternating isotactic *alt*-P3HBHp using the methyl-$^n$butyl disubstituted *rac*-8DLs (*RR*/*SS*-8DL$^{Me-Bu}$). Similarly, the polymerization by catalyst **1** was rather sluggish and offered poor sequence control, as indicated by Figure 3A-e. Catalysts **2** and **3** efficiently polymerized 100 equiv of monomer to completion in 30 min at 25 °C, yielding *alt*-P3HBHp with $M_n$ = 50.5 and 31.4 kDa (Table 1, runs 17 and 19) and some site-/stereo-errors (Figure 3A-f,g,B). Similarly, catalyst **4** with the bulky trityl-substituted ligand produced perfectly alternating isotactic *alt*-P3HBHp (Table 1, run 21), as indicated by the only two carbonyl peaks centered at 169.1 ppm and single peaks for the methylene carbons at 40.6 and 39.2 ppm (Figure 3A-h,B). Overall, the ROP studies on *RR*/*SS*-8DL$^{Me-Et/Bu}$ demonstrated that the unsymmetrical *rac*-8DL$^{R1-R2}$ is a promising platform for the access to alternating isotactic PHAs potentially possessing diverse and intriguing properties.

**Ring-Opening Site Selectivity.** The abovementioned ROP results demonstrated the successful synthesis of perfect isotactic *alt*-P3HBV(Hp) with high to quantitative alternation by site- and stereoselective ROP of *RR*/*SS*-8DL$^{Me-Et/Bu}$ with discrete chiral yttrium catalysts. However, these results brought up an interesting fundamental question: which site of the diester ring is exclusively opened during the ROP process? To answer this question, we first set up the reference chemical shifts by nonselectively opening the ring with acidified MeOH (5% v/v HCl), leading to the formation of two regio-isomeric products with different terminal groups that represent the two possible end groups of *alt*-P3HBV (Figure 4A). Through 2D $^1$H−$^1$H correlation spectroscopy (Figure S15), the two sets of $^1$H NMR signals centered at 4.05 and 3.80 ppm were assigned to the methyl-substituted and ethyl-substituted hydroxyl terminal groups, respectively. Next, isotactic *alt*-P3HBV with a relatively low molecular weight ($M_n$ = 6.5 kDa, $Đ$ = 1.19) produced by catalyst **4** was subjected to the comparison with the established $^1$H NMR reference, as shown in Figure 4B. The presence of the only observed methyl-substituted hydroxyl terminal group suggested that the ring-opening takes place exclusively at the methyl-substituted ester site (Figure 4B), which is consistent with previous literature showing that ring-opening occurs preferentially at the less hindered site.[38]

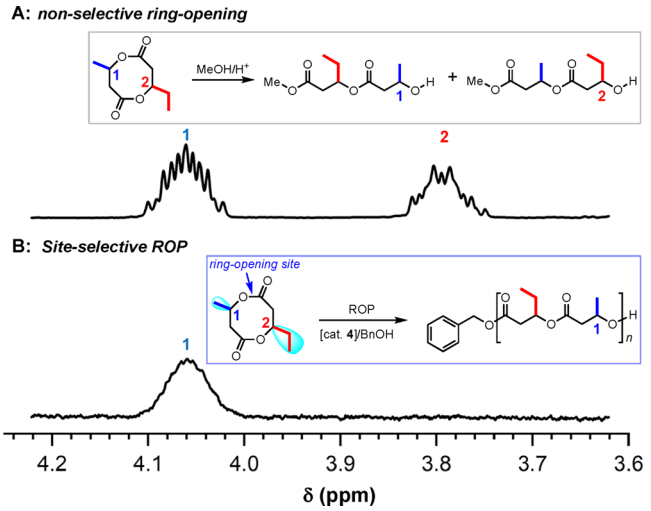


**Figure 4.** (A) $^1$H NMR spectrum of nonselectively ring-opened *RR*/*SS*-8DL$^{Me-Et}$ in the terminal methylene region. (B) $^1$H NMR spectrum of isotactic *alt*-P3HBV produced with catalyst **4** in a [monomer]/[catalyst]/[BnOH] ratio of 20:1:1, showing exclusive ring-opening at the $\alpha$-methyl ester site.

**Thermal and Mechanical Properties of *alt*-P3HBV-(Hp).** Thermal transition behaviors of isotactic *alt*-P3HBV prepared with catalysts **2** (**P1**), **3** (**P2**), and **4** (**P3**) under identical conditions (monomer/catalyst/BnOH = 200:1:1) were investigated with differential scanning calorimetry (DSC) and are compared in Figure 5A. To our surprise, **P1** and **P2**, the highly isotactic *alt*-P3HBV, are completely amorphous, displaying only observable glass transition temperature ($T_g$) at −6.9 and −9.5 °C, respectively, due to their imperfect (~80%) alternation. However, for **P3**, the perfectly alternating and isotactic copolymer, a much enhanced $T_g$ to −0.2 °C and a $T_m$ at 103.5 °C with a heat of fusion ($\Delta H_f$) value of 41.6 J g$^{-1}$ were observed, indicating a transition from amorphous (**P1** and **P2**) to semicrystalline PHA materials (**P3**) and highlighting the importance of the sequence- and stereoregularity of the polymer backbone on the resulting physical properties. Noticeably, DSC traces of the first cooling scan did not display any crystallization peak ($T_c$) and no $T_m$ was observed on the second heating scan even under a low heating/cooling rate of 1 °C min$^{-1}$ (Figures S16 and S17), all suggesting a slow crystallization process, presumably originated from the alternating nature of the polymer backbones, which is different from the fast crystallization behavior of the individual homopolymers.[36] On the other hand, isotactic *alt*-P3HBHp all appeared as liquid/wax-like materials, regardless of the sequence and stereoregularity. Even for **P4**, the one with the perfect backbone alternating sequence and isotacticity prepared with catalyst **4** ($M_n$ = 18.5 kDa, $Đ$ = 1.04), only a $T_g$ of −16.1 °C was observed, which is significantly lower than that of *alt*-P3HBV, as expected, due to the incorporation of the


https://doi.org/10.1021/jacs.2c08791
J. Am. Chem. Soc. 2022, 144, 20016−20024

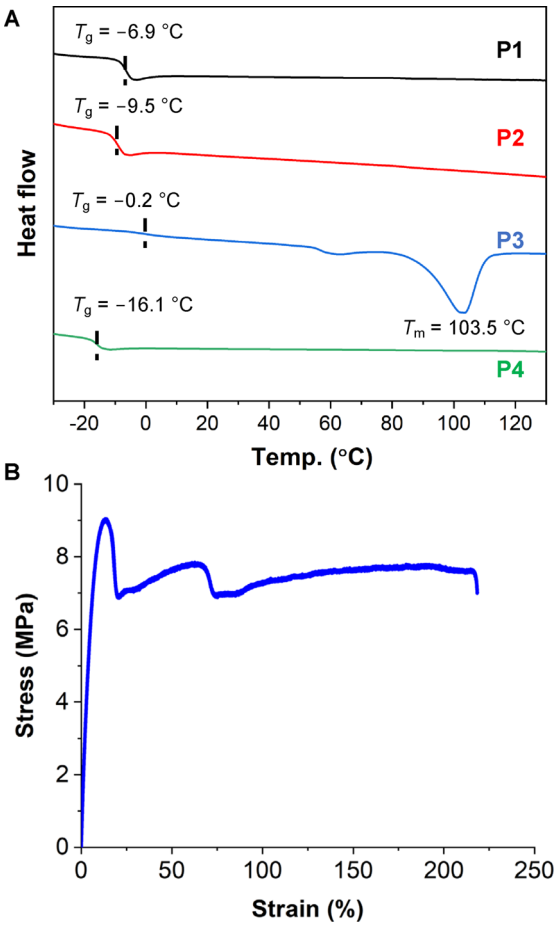


**Figure 5.** (A) DSC traces of *alt*-P3HBV materials prepared with catalysts **2** (**P1**), **3** (**P2**), and **4** (**P3**) in a [monomer]/[catalyst]/[BnOH] ratio of 200:1:1 and *alt*-P3HBHp (**P4**) prepared with catalyst **4** in a ratio of 100:1:1. Data collected from the first heating scan with a scan rate of 10 °C $min^{-1}$. (B) Stress−strain curve of *alt*-P3HBV prepared with catalyst **4** and 1,4-benzenedimethanol initiator in a [monomer]/[catalyst]/[initiator] ratio of 200:1:0.5 ($M_n$ = 70 kDa, $Đ$ = 1.02).

longer flexible butyl side chains that increase chain mobility and disrupt the packing of polymer backbones. Thermogravimetric analysis (TGA) of *alt*-P3HBV ($M_n$ = 30.7 kDa, $Đ$ = 1.01) prepared with catalyst **4** showed a decomposition temperature ($T_d$) (defined by the temperature of 5% weight loss in the TGA curve) of 246 °C and a maximum rate decomposition temperature ($T_{max}$) of 278 °C (Figure S18), offering a fairly large melt-processing window of 143 °C. Noticeably higher thermal stability was observed for *alt*-P3HBHp ($M_n$ = 18.5 KDa, $Đ$ = 1.04) prepared with catalyst **4**, displaying $T_d$ and $T_{max}$ of 254 and 290 °C, respectively (Figure S19).

Isotactic homopolymers P3HB and P3HV are known for their strong crystallization behavior, brittleness (∼3% elongation at break), and lack of optical clarity, which largely limit their potential applications. Considering the reduced crystallinity of *alt*-P3HBV, which could improve the melt-processability and mechanical performance, we synthesized *alt*-P3HBV ($M_n$ = 70 kDa, $Đ$ = 1.02) in a multi-gram scale using catalyst **4** combined with a 1,4-benzenedimethanol initiator in a [monomer]/[catalyst]/[initiator] ratio of 200:1:0.5. The polymer was processed into dog-bone-shaped test specimens (ASTM D638 standard; Type V) suitable for tensile testing via compression molding. Indeed, the obtained film is optically clear (Figure S20), and more significantly, the mechanical tests showed that *alt*-P3HBV is ductile with an ultimate strain (elongation at break) of up to 220% (Figure 5B).

**Enantiomeric (*R*)-*alt*-P3HBV and (*S*)-*alt*-P3HBV: Synthesis and Stereocomplexation.** Formation of supramolecular stereocomplexes between enantiomeric chiral polymer chains that dramatically changes the crystallization rate, crystallinity, and $T_m$ value of polymers, often leading to significantly enhanced thermal properties and distinct physical/mechanical properties, has been observed in various types of polyesters.[50−53] Apparently, an exception is P3HB, as physical blending of (*R*)-P3HB and (*S*)-P3HB did not yield a stereocomplex, that is, both the enantiomeric polymers and racemic mixtures display the same thermal/physical properties.[33] A rare example of stereocomplex formation observed in the broad poly(3-hydroxyalkanoate) family is a blend of enantiomeric isotactic poly(α-methyl-α-ethyl-β-propiolactone)s, where the blend exhibits a $T_m$ of ∼40 °C higher than those of enantiomeric polymers.[54,55] To explore how the alternating nature of *alt*-P3HBV, where the methyl and ethyl groups are not attached to the same α-carbon but to the α- and β-carbon in alternation, affects the stereocomplexation, we set out to synthesize (*R*)-*alt*-P3HBV and (*S*)-*alt*-P3HBV by employing enantiomerically pure catalysts (*S*,*S*)-**4** and (*R*,*R*)-**4**,[33] respectively (Scheme 2).

The enantioselective ROP of *RR*/*SS*-8DL$^{Me-Et}$ was carried out with a [monomer]/[(*R*,*R*)/(*S*,*S*)-**4**]/[BnOH] ratio of 200/1/1 at −30 °C (Table 1, runs 15 and 16). The kinetically resolved ROP of the racemic monomers and resulting

**Scheme 2. Enantioselective ROP for Kinetic Resolution of *RR*/*SS*-8DL$^{Me-Et}$ to (*R*)-*alt*-P3HBV and (*S*)-*alt*-P3HBV**

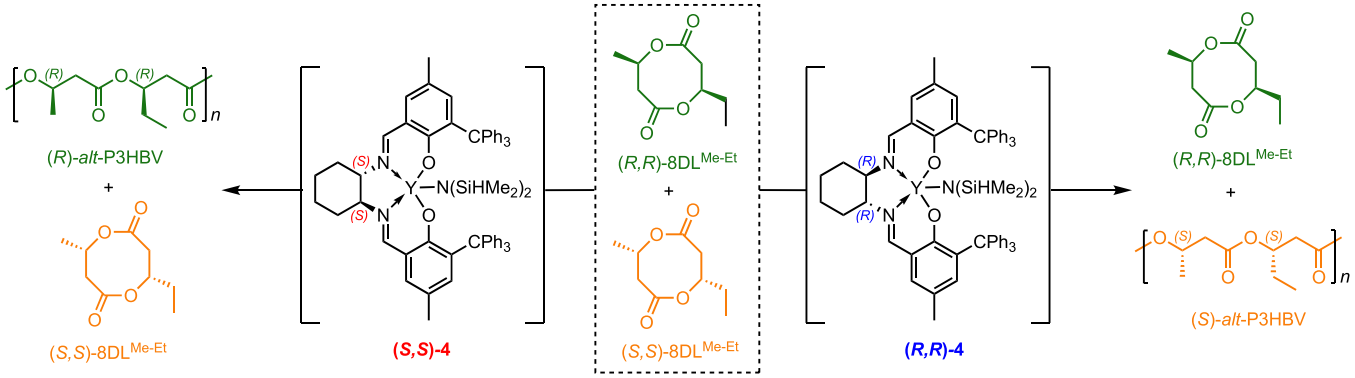




https://doi.org/10.1021/jacs.2c08791
J. Am. Chem. Soc. 2022, 144, 20016−20024

enantiomeric isotactic *alt*-P3HBV were confirmed by the following three lines of corroborative evidence. First, different from the ROP by *rac*-**4** with a 200-equiv. monomer loading that achieved quantitative conversion in 30 min, (*R*,*R*)-**4** and (*S*,*S*)-**4** only polymerized 50% monomer in 30 min, and extending reaction time to even 120 min did not further enhance the conversion (Figures S21−23), indicating exclusive catalyst site selectivity for one particular enantiomer of the monomer during the ROP process; this observation is identical to the enantioselective polymerization of the symmetrically substituted diolide *rac*-8DL$^{Me}$.[33] Second, the unreacted monomers displayed identical $^{1}$H NMR spectra (Figures S24 and 25) to the racemic mixture and the isolated polymers are perfectly isotactic, as evidenced by $^{13}$C NMR (Figures S26 and 27). Third, the 50% unreacted monomer produced by the ROP with (*R*,*R*)-**4** showed a specific rotation of −82.1°, while the specific rotation of the unreacted monomer obtained from the ROP with (*S*,*S*)-**4** was +80.0°, which were assigned to (*R*,*R*)-8DL$^{Me-Et}$ and (*S*,*S*)-8DL$^{Me-Et}$, respectively, according to our previous studies.[33] Overall, the presented evidence indicated that (*R*,*R*)-**4** selectively polymerized (*S*,*S*)-8DL$^{Me-Et}$, while (*S*,*S*)-**4** only polymerized (*R*,*R*)-8DL$^{Me-Et}$, which is coupled with perfect site selectivity for each ester site of monomers.

Intriguingly, enantiomeric (*R*)-*alt*-P3HBV and (*S*)-*alt*-P3HBV showed markedly different thermal properties and crystallization behavior than their 1:1 physical blend (Figure 6). DSC curves for the first heating scans (Figure 6A) of the enantiomeric polymers displayed a $T_m$ peak at 62.0 °C (heat of fusion $\Delta H_m$ = 35.7 to 39.8 J g$^{-1}$), but the 1:1 blend displayed a much higher $T_m$ of 114.6 °C and a $\Delta H_m$ of 50.1 J g$^{-1}$, which indicate a higher degree of crystallinity in the blend as a result of stereocomplexion. Powder XRD profiles (Figure 6B) of (*R*)-*alt*-P3HBV and (*S*)-*alt*-P3HBV exhibited almost identical crystalline diffraction patterns, consisting of four major peaks located at 2$\theta$ = 12.1°, 15.1°, 18.4°, and 20.5° and a few minor signals at higher 2$\theta$ values. In comparison, three of the major peaks (2$\theta$ =12.1°, 15.1°, and 18.4°) presented in the enantiomers were absent in the 1:1 blend and two new pronounced peaks at 2$\theta$ = 13.4° and 16.7° emerged, which are again attributed to the stereocomplex formation. As expected, the *alt*-P3HBV synthesized with catalyst *rac*-**4** displayed a $T_m$ similar to, and the XRD profile same as, the blend prepared by mixing equal amounts of (*R*) and (*S*)-*alt*-P3HBV (Figure S28), indicating the formation of a stereocomplex between chains of different chiralities produced by the racemic catalyst. It is worth noting that both the enantiomers and the blend displayed rather similar Fourier transform infrared spectra (Figure S29) with no noticeable shift of the C=O stretching frequency ($\nu_{C=O}$) observed; this is presumably due to the relatively weak complexation interaction between the two enantiomeric polymers so that the impact on the C=O stretching frequency was not noticeably observed, unlike the more pronounced effect observable on the crystallization behavior.

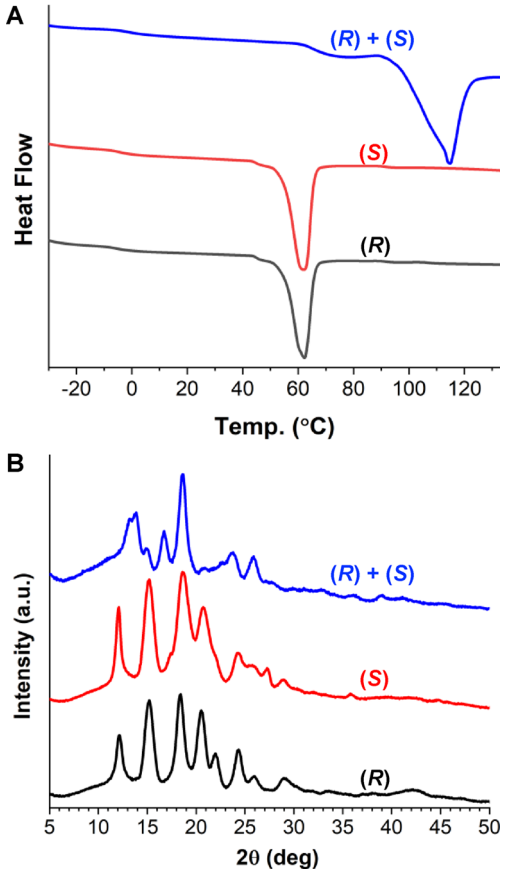


**Figure 6.** (A) DSC curves of the first heating scan; scan rate = 10 °C min$^{-1}$. (B) Powder XRD profiles of (*R*)-*alt*-P3HBV and (*S*)-*alt*-P3HBV and their 1:1 physical blend.

## CONCLUSIONS

In summary, we reported here the synthesis of perfectly alternating, isotactic PHAs via ROP of unsymmetrically substituted *rac*-8DLs catalyzed by discrete, chiral yttrium complexes, one of which (the bulky trityl-substituted catalyst **4**) exhibits essentially quantitative site and stereoselectivity. This synthesis was realized by monomer's structural design and rationalized manipulations of the steric interplay/matching between the structure and chirality of monomers and catalysts. Mechanistic investigation showed exclusive ring-opening occurring at the less sterically hindered $\alpha$-methyl-substituted ester site, accounting for the observed perfect site selectivity, thus perfect alternating Me/Et sequences along the polymer backbone. The resulting unique alternating isotactic PHA materials display significantly different thermal/physical properties as a function of the site and stereoregularity of the polymer backbones. In sharp contrast to the individual isotactic homopolymers P3HB and P3HV, alternating isotactic copolymer *alt*-P3HBV displays substantially improved mechanical properties, with an elongation at break of 220% (vs <10% for isotactic P3HB or P3HV). Kinetically resolved ROP of *RR*/*SS*-8DL$^{Me-Et}$ with enantiomeric (*R*,*R*) and (*S*,*S*)-**4** led to (*S*)-*alt*-P3HBV and (*R*)-*alt*-P3HBV, respectively. These enantiomeric PHAs were found to form a stereocomplex, as evidenced by the enhanced $T_m$ (by 53 °C) and different XRD profiles, whereas this stereocomplexation phenomenon was not observed in the individual homopolymers. In fact, this represents a rare example of stereocomplex formation in the PHA family and suggests another unique feature brought about by the perfectly alternating structure.

This study further expands the utility of the 8DL monomer family as a promising platform for accessing a variety of novel PHA materials, including the novel alternating isotactic PHAs reported herein. By rational design of unsymmetric monomers and chiral catalysts as well as judicious selection of proper


https://doi.org/10.1021/jacs.2c08791
J. Am. Chem. Soc. 2022, 144, 20016−20024

reaction conditions, other emerging alternating PHA materials with tailored physical/mechanical properties and potentially useful functionalities could be discovered, thereby opening up new opportunities for synthetic designer PHAs.

## ■ ASSOCIATED CONTENT

### Supporting Information

The Supporting Information is available free of charge at https://pubs.acs.org/doi/10.1021/jacs.2c08791.

Experimental details, monomer and polymer syntheses, and characterization data (PDF)

### Accession Codes

CCDC 2190188 contains the supplementary crystallographic data for this paper. These data can be obtained free of charge via www.ccdc.cam.ac.uk/data_request/cif, or by emailing data_request@ccdc.cam.ac.uk, or by contacting The Cambridge Crystallographic Data Centre, 12 Union Road, Cambridge CB2 1EZ, UK; fax: +44 1223 336033.

## ■ AUTHOR INFORMATION


### Corresponding Author

**Eugene Y.-X. Chen** − *Department of Chemistry, Colorado State University, Fort Collins, Colorado 80523-1872, United States;* orcid.org/0000-0001-7512-3484; Email: eugene.chen@colostate.edu

### Authors

**Zhen Zhang** − *Department of Chemistry, Colorado State University, Fort Collins, Colorado 80523-1872, United States*

**Changxia Shi** − *Department of Chemistry, Colorado State University, Fort Collins, Colorado 80523-1872, United States*

**Miriam Scoti** − *Department of Chemistry, Colorado State University, Fort Collins, Colorado 80523-1872, United States; Dipartimento di Scienze Chimiche, Università di Napoli Federico II, Napoli 80126, Italy;* orcid.org/0000-0001-9225-1509

**Xiaoyan Tang** − *Department of Chemistry, Colorado State University, Fort Collins, Colorado 80523-1872, United States;* orcid.org/0000-0002-0050-6699

Complete contact information is available at: https://pubs.acs.org/10.1021/jacs.2c08791


### Notes

The authors declare no competing financial interest.

## ■ ACKNOWLEDGMENTS

We gratefully acknowledge support by the U.S. Department of Energy, Office of Energy Efficiency and Renewable Energy, Advanced Manufacturing Office (AMO) and Bioenergy Technologies Office (BETO). This work was performed as part of the BOTTLE Consortium and funded under contract no. DE-AC36-08GO28308 with the National Renewable Energy Laboratory, operated by Alliance for Sustainable Energy. In the early stage of the PHA project, the work was supported by the U.S. National Science Foundation (NSF-1955482).

## ■ REFERENCES


(1) Adeleye, A. T.; Odoh, C. K.; Enudi, O. C.; Banjoko, O. O.; Osiboye, O. O.; Odediran, E. T.; Louis, H. Sustainable synthesis and applications of polyhydroxyalkanoates (PHAs) from biomass. *Process Biochem.* **2020**, *96*, 174−193.

(2) Anjum, A.; Zuber, M.; Zia, K. M.; Noreen, A.; Anjum, M. N.; Tabasum, S. Microbial production of polyhydroxyalkanoates (PHAs) and its copolymers: a review of recent advancements. *Int. J. Biol. Macromol.* **2016**, *89*, 161−174.

(3) Chen, G.-Q. A microbial polyhydroxyalkanoates (PHA) based bio-and materials industry. *Chem. Soc. Rev.* **2009**, *38*, 2434−2446.

(4) Lenz, R. W.; Marchessault, R. H. Bacterial polyesters: biosynthesis, biodegradable plastics and biotechnology. *Biomacromolecules* **2005**, *6*, 1−8.

(5) Muhammadi; Shabina; Afzal, M.; Hameed, S. Bacterial polyhydroxyalkanoates-eco-friendly next generation plastic: production, biocompatibility, biodegradation, physical properties and applications. *Green Chem. Lett. Rev.* **2015**, *8*, 56−77.

(6) Müller, H. M.; Seebach, D. Poly (hydroxyalkanoates): a fifth class of physiologically important organic biopolymers? *Angew. Chem., Int. Ed.* **1993**, *32*, 477−502.

(7) Poirier, Y.; Nawrath, C.; Somerville, C. Production of polyhydroxyalkanoates, a family of biodegradable plastics and elastomers, in bacteria and plants. *Nat. Biotechnol.* **1995**, *13*, 142−150.

(8) Raza, Z. A.; Abid, S.; Banat, I. M. Polyhydroxyalkanoates: Characteristics, production, recent developments and applications. *Int. Biodeterior. Biodegrad.* **2018**, *126*, 45−56.

(9) Reddy, C.; Ghai, R.; Kalia, V. C. Polyhydroxyalkanoates: an overview. *Bioresour. Technol.* **2003**, *87*, 137−146.

(10) Somleva, M. N.; Peoples, O. P.; Snell, K. D. PHA bioplastics, biochemicals, and energy from crops. *Plant Biotechnol. J.* **2013**, *11*, 233−252.

(11) Sudesh, K.; Abe, H.; Doi, Y. Synthesis, structure and properties of polyhydroxyalkanoates: biological polyesters. *Prog. Polym. Sci.* **2000**, *25*, 1503−1555.

(12) Chen, G.; Zhang, G.; Park, S.; Lee, S. Industrial scale production of poly (3-hydroxybutyrate-co-3-hydroxyhexanoate). *Appl. Microbiol. Biotechnol.* **2001**, *57*, 50−55.

(13) Kramer, J. W.; Treitler, D. S.; Dunn, E. W.; Castro, P. M.; Roisnel, T.; Thomas, C. M.; Coates, G. W. Polymerization of enantiopure monomers using syndiospecific catalysts: a new approach to sequence control in polymer synthesis. *J. Am. Chem. Soc.* **2009**, *131*, 16042−16044.

(14) Ligny, R.; Guillaume, S. M.; Carpentier, J. F. Yttrium-Mediated Ring-Opening Copolymerization of Oppositely Configurated 4-Alkoxymethylene-β-Propiolactones: Effective Access to Highly Alternated Isotactic Functional PHAs. *Chem. − Eur. J.* **2019**, *25*, 6412−6424.

(15) Shakaroun, R. M.; Jehan, P.; Alaaeddine, A.; Carpentier, J.-F.; Guillaume, S. M. Organocatalyzed ring-opening polymerization (ROP) of functional β-lactones: new insights into the ROP mechanism and poly (hydroxyalkanoate) s (PHAs) macromolecular structure. *Polym. Chem.* **2020**, *11*, 2640−2652.

(16) Tang, X.; Shi, C.; Zhang, Z.; Chen, E. Y.-X. Toughening Biodegradable Isotactic Poly (3-hydroxybutyrate) via Stereoselective Copolymerization of a Diolide and Lactones. *Macromolecules* **2021**, *54*, 9401−9409.

(17) Westlie, A. H.; Chen, E. Y.-X. Catalyzed chemical synthesis of unnatural aromatic polyhydroxyalkanoate and aromatic−aliphatic PHAs with record-high glass-transition and decomposition temperatures. *Macromolecules* **2020**, *53*, 9906−9915.

(18) Yang, J. C.; Yang, J.; Li, W. B.; Lu, X. B.; Liu, Y. Carbonylative Polymerization of Epoxides Mediated by Tri-metallic Complexes: A Dual Catalysis Strategy for Synthesis of Biodegradable Polyhydroxyalkanoates. *Angew. Chem., Int. Ed.* **2022**, *61*, No. e202116208.

(19) Zhang, X.; Fevre, M.; Jones, G. O.; Waymouth, R. M. Catalysis as an enabling science for sustainable polymers. *Chem. Rev.* **2018**, *118*, 839−885.

(20) Carpentier, J.-F. Rare-earth complexes supported by tripodal tetradentate bis (phenolate) ligands: a privileged class of catalysts for ring-opening polymerization of cyclic esters. *Organometallics* **2015**, *34*, 4175−4189.

(21) Badi, N.; Lutz, J.-F. Sequence control in polymer synthesis. *Chem. Soc. Rev.* **2009**, *38*, 3383−3390.

(22) Geng, K.; Tsui, O. K. Effects of polymer tacticity and molecular weight on the glass transition temperature of poly (methyl methacrylate) films on silica. *Macromolecules* **2016**, *49*, 2671−2678.
(23) Jones, T. D.; Chaffin, K. A.; Bates, F. S.; Annis, B.; Hagaman, E.; Kim, M.-H.; Wignall, G. D.; Fan, W.; Waymouth, R. Effect of tacticity on coil dimensions and thermodynamic properties of polypropylene. *Macromolecules* **2002**, *35*, 5061−5068.
(24) Lutz, J.-F.; Neugebauer, D.; Matyjaszewski, K. Stereoblock copolymers and tacticity control in controlled/living radical polymerization. *J. Am. Chem. Soc.* **2003**, *125*, 6986−6993.
(25) Perry, S. L.; Sing, C. E. 100th anniversary of macromolecular science viewpoint: Opportunities in the physics of sequence-defined polymers. *ACS Macro Lett.* **2020**, *9*, 216−225.
(26) Zintl, M.; Molnar, F.; Urban, T.; Bernhart, V.; Preishuber-Pflügl, P.; Rieger, B. Variably Isotactic Poly (hydroxybutyrate) from Racemic β-Butyrolactone: Microstructure Control by Achiral Chromium (III) Salophen Complexes. *Angew. Chem., Int. Ed.* **2008**, *47*, 3458−3460.
(27) Ajellal, N.; Bouyahyi, M.; Amgoune, A.; Thomas, C. M.; Bondon, A.; Pillin, I.; Grohens, Y.; Carpentier, J.-F. Syndiotactic-enriched poly (3-hydroxybutyrate) s via stereoselective ring-opening polymerization of racemic β-butyrolactone with discrete yttrium catalysts. *Macromolecules* **2009**, *42*, 987−993.
(28) Amgoune, A.; Thomas, C. M.; Ilinca, S.; Roisnel, T.; Carpentier, J. F. Highly active, productive, and syndiospecific yttrium initiators for the polymerization of racemic β-butyrolactone. *Angew. Chem., Int. Ed.* **2006**, *45*, 2782−2784.
(29) Chamberlain, B. M.; Cheng, M.; Moore, D. R.; Ovitt, T. M.; Lobkovsky, E. B.; Coates, G. W. Polymerization of lactide with zinc and magnesium β-diiminate complexes: stereocontrol and mechanism. *J. Am. Chem. Soc.* **2001**, *123*, 3229−3238.
(30) Cheng, M.; Attygalle, A. B.; Lobkovsky, E. B.; Coates, G. W. Single-site catalysts for ring-opening polymerization: Synthesis of heterotactic poly (lactic acid) from rac-lactide. *J. Am. Chem. Soc.* **1999**, *121*, 11583−11584.
(31) Kerr, R. W.; Williams, C. K. Zr (IV) Catalyst for the Ring-Opening Copolymerization of Anhydrides (A) with Epoxides (B), Oxetane (B), and Tetrahydrofurans (C) to Make ABB-and/or ABC-Poly (ester-alt-ethers). *J. Am. Chem. Soc.* **2022**, *144*, 6882−6893.
(32) Li, H.; Ollivier, J.; Guillaume, S. M.; Carpentier, J. F. Tacticity Control of Cyclic Poly (3-Thiobutyrate) Prepared by Ring-Opening Polymerization of Racemic β-Thiobutyrolactone. *Angew. Chem., Int. Ed.* **2022**, *61*, No. e202202386.
(33) Tang, X.; Chen, E. Y.-X. Chemical synthesis of perfectly isotactic and high melting bacterial poly (3-hydroxybutyrate) from bio-sourced racemic cyclic diolide. *Nat. Commun.* **2018**, *9*, 2345.
(34) Carpentier, J. F. Discrete metal catalysts for stereoselective ring-opening polymerization of chiral racemic β-lactones. *Macromol. Rapid Commun.* **2010**, *31*, 1696−1705.
(35) Li, H.; Shakaroun, R. M.; Guillaume, S. M.; Carpentier, J. F. Recent Advances in Metal-Mediated Stereoselective Ring-Opening Polymerization of Functional Cyclic Esters towards Well-Defined Poly (hydroxy acid) s: From Stereoselectivity to Sequence-Control. *Chem. − Eur. J.* **2020**, *26*, 128−138.
(36) Tang, X.; Westlie, A. H.; Watson, E. M.; Chen, E. Y.-X. Stereosequenced crystalline polyhydroxyalkanoates from diastereomeric monomer mixtures. *Science* **2019**, *366*, 754−758.
(37) Jaffredo, C. G.; Chapurina, Y.; Guillaume, S. M.; Carpentier, J. F. From syndiotactic homopolymers to chemically tunable alternating copolymers: Highly active Yttrium complexes for stereoselective ring-opening polymerization of β-Malolactonates. *Angew. Chem., Int. Ed.* **2014**, *53*, 2687−2691.
(38) Lu, Y.; Swisher, J. H.; Meyer, T. Y.; Coates, G. W. Chirality-Directed Regioselectivity: An Approach for the Synthesis of Alternating Poly (Lactic-co-Glycolic Acid). *J. Am. Chem. Soc.* **2021**, *143*, 4119−4124.
(39) Jia, Z.; Jiang, J.; Zhang, X.; Cui, Y.; Chen, Z.; Pan, X.; Wu, J. Isotactic-alternating, heterotactic-alternating, and ABAA-type sequence-controlled copolyester syntheses via highly stereoselective and regioselective ring-opening polymerization of cyclic diesters. *J. Am. Chem. Soc.* **2021**, *143*, 4421−4432.
(40) Hodge, P. Entropically driven ring-opening polymerization of strainless organic macrocycles. *Chem. Rev.* **2014**, *114*, 2278−2312.
(41) Naumann, S.; Thomas, A. W.; Dove, A. P. Highly polarized alkenes as organocatalysts for the polymerization of lactones and trimethylene carbonate. *ACS Macro Lett.* **2016**, *5*, 134−138.
(42) Takwa, M.; Xiao, Y.; Simpson, N.; Malmström, E.; Hult, K.; Koning, C. E.; Heise, A.; Martinelle, M. Lipase catalyzed HEMA initiated ring-opening polymerization: In situ formation of mixed polyester methacrylates by transesterification. *Biomacromolecules* **2008**, *9*, 704−710.
(43) Hong, M.; Chen, E. Y.-X. Completely recyclable biopolymers with linear and cyclic topologies via ring-opening polymerization of γ-butyrolactone. *Nat. Chem.* **2016**, *8*, 42−49.
(44) Hong, M.; Tang, X.; Newell, B. S.; Chen, E. Y.-X. "Nonstrained" γ-butyrolactone-based copolyesters: copolymerization characteristics and composition-dependent (thermal, eutectic, cocrystallization, and degradation) properties. *Macromolecules* **2017**, *50*, 8469−8479.
(45) Tang, X.; Hong, M.; Falivene, L.; Caporaso, L.; Cavallo, L.; Chen, E. Y.-X. The quest for converting biorenewable bifunctional α-methylene-γ-butyrolactone into degradable and recyclable polyester: controlling vinyl-addition/ring-opening/cross-linking pathways. *J. Am. Chem. Soc.* **2016**, *138*, 14326−14337.
(46) Anwander, R.; Runte, O.; Eppinger, J.; Gerstberger, G.; Herdtweck, E.; Spiegler, M. Synthesis and structural characterisation of rare-earth bis (dimethylsilyl) amides and their surface organometallic chemistry on mesoporous MCM-41. *J. Chem. Soc., Dalton Trans.* **1998**, 847−858.
(47) Eppinger, J.; Herdtweck, E.; Anwander, R. Synthesis and characterization of alkali metal bis (dimethylsilyl) amides: infinite all-planar laddering in the unsolvated sodium derivative. *Polyhedron* **1998**, *17*, 1195−1201.
(48) Dubois, P.; Jacobs, C.; Jérôme, R.; Teyssie, P. Macromolecular engineering of polylactones and polylactides. 4. Mechanism and kinetics of lactide homopolymerization by aluminum isopropoxide. *Macromolecules* **1991**, *24*, 2266−2270.
(49) Stridsberg, K.; Albertsson, A. C. Ring-opening polymerization of 1, 5-dioxepan-2-one initiated by a cyclic tin-alkoxide initiator in different solvents. *J. Polym. Sci., Polym. Chem.* **1999**, *37*, 3407−3417.
(50) Brochu, S.; Prud'Homme, R. E.; Barakat, I.; Jerome, R. Stereocomplexation and morphology of polylactides. *Macromolecules* **1995**, *28*, 5230−5239.
(51) Popowski, Y.; Lu, Y.; Coates, G. W.; Tolman, W. B. Stereocomplexation of Stereoregular Aliphatic Polyesters: Change from Amorphous to Semicrystalline Polymers with Single Stereocenter Inversion. *J. Am. Chem. Soc.* **2022**, *144*, 8362−8370.
(52) Wan, Z.-Q.; Longo, J. M.; Liang, L.-X.; Chen, H.-Y.; Hou, G.-J.; Yang, S.; Zhang, W.-P.; Coates, G. W.; Lu, X.-B. Comprehensive understanding of polyester stereocomplexation. *J. Am. Chem. Soc.* **2019**, *141*, 14780−14787.
(53) Zhu, J.-B.; Watson, E. M.; Tang, J.; Chen, E. Y.-X. A synthetic polymer system with repeatable chemical recyclability. *Science* **2018**, *360*, 398−403.
(54) Lavallee, C.; Prud'Homme, R. E. Stereocomplexation of isotactic polyesters of opposite configurations. *Macromolecules* **1989**, *22*, 2438−2446.
(55) Grenier, D.; Prud'Homme, R. E. Complex formation between enantiomeric polyesters. *J. Polym. Sci., Polym. Phys. Ed.* **1984**, *22*, 577−587.


https://doi.org/10.1021/jacs.2c08791
J. Am. Chem. Soc. 2022, 144, 20016−20024